Advanced signal processing for integrated LES-RANS simulations: Anti-aliasing filters

By J. U. Schlüter

1. Motivation

Currently, a wide variety of flow phenomena are addressed with numerical simulations. Many flow solvers are optimized to simulate a limited spectrum of flow effects effectively, such as single parts of a flow system, but are either inadequate or too expensive to be applied to a very complex problem.

As an example, the flow through a gas turbine can be considered. In the compressor and the turbine section, the flow solver has to be able to handle the moving blades, model the wall turbulence, and predict the pressure and density distribution properly. This can be done by a flow solver based on the Reynolds-Averaged Navier-Stokes (RANS) approach (Davis *et al.* 2002). On the other hand, the flow in the combustion chamber is governed by large scale turbulence, chemical reactions, and the presence of fuel spray. Experience shows that these phenomena require an unsteady approach (Veynante and Poinsot 1996). Hence, for the combustor, the use of a Large Eddy Simulation (LES) flow solver is desirable (Mahesh *et al.* 2001; Constantinescu *et al.* 2003).

While many design problems of a single flow passage can be addressed by separate computations, only the simultaneous computation of all parts can guarantee the proper prediction of multi-component phenomena, such as compressor/combustor instability and combustor/turbine hot-streak migration. Therefore, a promising strategy to perform full aero-thermal simulations of gas-turbine engines is the use of a RANS flow solver for the compressor sections, an LES flow solver for the combustor, and again a RANS flow solver for the turbine section (Fig. 1).

2. Interface Conditions

The simultaneous computation of the flow in all parts of a gas turbine with different flow solvers requires an exchange of information at the interfaces of the computational domains of each part. Previous work has established algorithms, which ensure that two or more simultaneously running flow solvers are able to exchange the information at the interfaces efficiently (Shankaran *et al.* 2001; Schlüter *et al.* 2003d).

The necessity of information exchange in the flow direction from the upstream to the downstream flow solver is obvious: the flow in a passage is strongly dependent on mass flux, velocity vectors, and temperature at the inlet of the domain. However, since the Navier-Stokes equations are elliptic in subsonic flows, the downstream flow conditions can have a substantial influence on the upstream flow development. This can easily be imagined by considering that, for instance, a flow blockage in the turbine section of the gas turbine can determine and even stop the mass flow rate through the entire engine. This means that the information exchange at each interface has to go in both, downstream *and* upstream, directions.

Considering an LES flow solver computing the flow in the combustor, information on

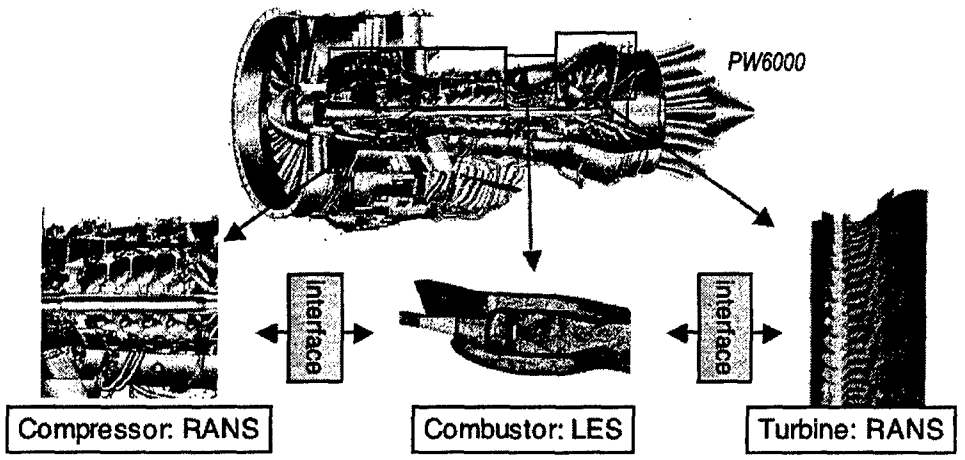

FIGURE 1. Decomposition of gas turbine engine. LES of combustor from Mahesh *et al.* 2001; Constantinescu *et al.* 2003, RANS of turbine section from Davis *et al.* 2002

the flow field has to be provided to the RANS flow solver computing the turbine as well as to the RANS flow solver computing the compressor. At the same time, the LES solver has to obtain flow information from both RANS flow solvers. The coupling can be done using overlapping computational domains for the LES and RANS simulations. For the example of the compressor/combustor interface this would imply that inflow conditions for LES will be determined from the RANS solution at the beginning of the overlap region, and correspondingly the outflow conditions for RANS are determined from the LES solution at the end of the overlap region.

However, the different mathematical approaches of the different flow solvers make the coupling of the flow solvers challenging. Since LES resolves large-scale turbulence in space and time, the time step between two iterations is relatively small. RANS flow solvers average all turbulent motions over time and predict ensemble averages of the flow. Even when a so-called unsteady RANS approach is used, the time step between two ensemble-averages of the RANS flow solver is usually larger by several orders of magnitude than that for an LES flow solver.

The smaller time-step of the LES flow solver results in the necessity of the LES flow solver to average its own LES data over the RANS time-step in order to provide data for the RANS flow solver at the requested times. However, the sampling process may introduce errors in the frequency spectra.

As an analogy, the digitization of an continuous signal during experiments can be seen. Here, the highest frequency recorded without error is the Nyquist frequency, defined as half of the sampling frequency. Low pass filters are used in order to remove high frequency disturbances from the continuous signal before the sampling process. Omitting the filtering would result in aliasing errors, which means that under-resolved frequencies ($f > f_{\text{NYQUIST}}$) are found in the long wave spectrum. Hence, the low-pass filtering *prior* to the digitization is necessary.

For the communication between LES and RANS flow solvers a similar procedure has to be found in order to avoid aliasing of frequencies in the sampling of the LES data. The current study investigates the use of filters to ensure the proper communication of flow variables.

3. Interface Implementation and Flow Solver

For the present study, the information transfer between two flow solvers has been studied. The idea is to periodically excite the flow in the upstream domain and observe the information transfer to the downstream domain. To be able to compare with the true solution of a simulation of the entire domain with a single code, this study has been done by coupling two instances of the same flow solver. Both LES flow solvers exchange information at a time step $\Delta\tau$, which is larger by more than one order of magnitude than the LES time step Δt.

The LES flow solver developed at the Center for Turbulence Research (Pierce & Moin 1998) has been used. The flow solver solves the filtered momentum equations with a low-Mach number assumption on an axi-symmetric structured mesh. A second-order finite-volume scheme on a staggered grid is used (Akselvoll & Moin 1996).

The sub-grid stresses are approximated with an eddy-viscosity approach. The eddy viscosity is determined by a dynamic procedure (Germano *et al.* 1991; Moin *et al.* 1991).

For the real-time exchange of flow variables during the simultaneous computation of both domains, a recently developed interface has been used (Schlüter *et al.* 2002; Schlüter *et al.* 2003d). The interface establishes a communication between the two flow solvers and lets the flow solvers exchange flow variables after a given time-step $\Delta\tau$. Each of the flow solvers obtains a data set of flow variables for each point at the boundary. Then, each flow solver defines its own boundary conditions from the data obtained. At the inlet of the downstream LES flow solver, inflow boundary conditions corresponding to Schlüter *et al.* (2003b) (see also Schlüter *et al.* 2003a; Schlüter 2003) have been employed.

Previous work has shown that at the outflow of the upstream domain outlet boundary conditions have to be employed taking the feedback from the downstream domain into account (Schlüter and Pitsch 2001; Schlüter *et al.* 2002; Schlüter *et al.* 2003c). This can be done by employing a body force near the outlet of the domain, which drives the flow to a solution given by the flow solution of the downstream domain. However, in the current case the feedback was consciously suppressed. This was done to avoid that aliased frequencies received by the downstream domain are given back to the upstream domain and may contaminate the outgoing signal from the upstream domain. This means that if the feedback is not suppressed, the numerical error due to aliasing may even increase. The suppression ensures that all effects of variations of the interface can be associated directly with the filter change. Since there is no feedback from the downstream flow solver, the time-evolving LES solution of the upstream flow solver is identical for all cases reported here.

The inlet boundary condition of the *upstream* domain has been determined by:

$$u_{i,\mathrm{LES}}(t) = \bar{u}_{i,\mathrm{MEAN}}(t) + u'_{i,\mathrm{DB}}(t) \tag{3.1}$$

where t the time using the LES time scale and $u'_{i,\mathrm{DB}}(t)$ is a turbulent motion from a pre-generated data-base. In laminar cases the turbulent fluctuation was set to zero. For turbulent cases, the mean flow-field at the inlet and the data-base for the turbulent motions were determined by a separate LES computation of a weakly swirling periodic pipe flow. The swirl number of this pipe flow was $S = 0.15$ with:

$$S = \frac{1}{D}\frac{\int_0^D r^2 \bar{u}_x \bar{u}_\phi \, dr}{\int_0^D r \bar{u}_x^2 \, dr}, \tag{3.2}$$

where u_x is the axial velocity component, u_ϕ is the azimuthal velocity component, and D is the diameter of the pipe.

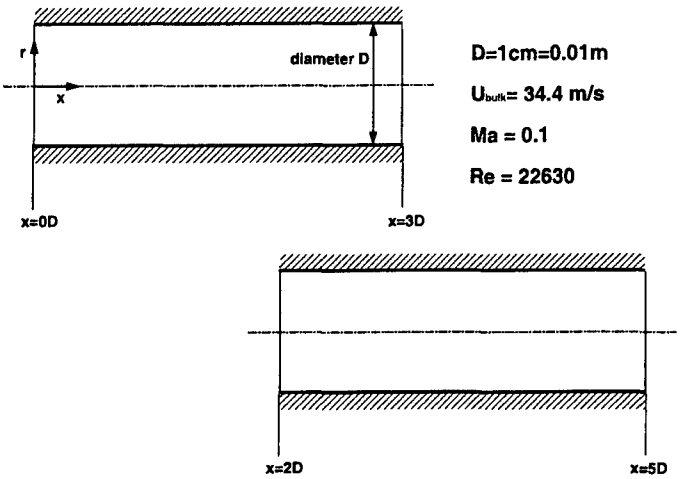

FIGURE 2. Geometry of the test-case.

In order to simulate a convective wave, the azimuthal velocity component has been modulated by:

$$\bar{u}_{\phi,\mathrm{MEAN}}(t) = \bar{u}_{\phi,\mathrm{DB}} \cdot [1.0 + 0.3 \cdot \sin(2\pi \cdot St \cdot t)] \tag{3.3}$$

with $\bar{u}_{\phi,\mathrm{DB}}$ the mean velocity of the data-base.

4. Aliasing Problem

In order to investigate the aliasing problem in integrated LES-RANS computations consider the following case: a pipe is split into an upstream domain computed by one flow solver and a downstream domain computed by another flow solver. Both pipe segments are 3 diameters D long with an overlap of $1D$ (Fig. 2). The upstream flow domain possesses two dominant frequencies, one at a Strouhal number $St = 1.0$ with $St = fD/U_{\mathrm{bulk}}$ and another at $St = 7.5$. The interface frequency is set to $St = 10.0$, which leads to a Nyquist frequency of $St = 5.0$. Hence, the long wave frequency at $St = 1.0$ is well resolved and can be transmitted to the downstream domain. However, the second frequency is under-resolved and will lead to aliasing errors.

To demonstrate this, such a flow calculation was performed under laminar conditions at a Reynolds-number $Re = 1000$. Laminar conditions have been chosen for clarity. A turbulent flow is examined below.

Figure 3 shows the energy spectrum in the upstream domain at a point in the interface plane ($x = 2D$, $r = 0.5R$, $\phi = 0$). The two distinct peaks can be associated with the forcing frequencies. A successful signal processing will transfer the low frequency ($St = 1.0$) with no energy loss, while suppressing the high frequency disturbance ($St = 7.5$).

Figure 4 shows the energy spectrum for the same physical point, but in the downstream domain. Since the flow solver computing the upstream domain has transferred the signal without any treatment, the high frequency perturbation in the upstream domain has been aliased and can now be found as a spurious contribution at a lower frequency of $St = 2.5$.

This may cause considerable problems, since this frequency is resolved by any unsteady RANS flow solver operating at a time-step correspondent to the interface frequency. Since this peak in the long wave spectrum is not present in the upstream domain, this error

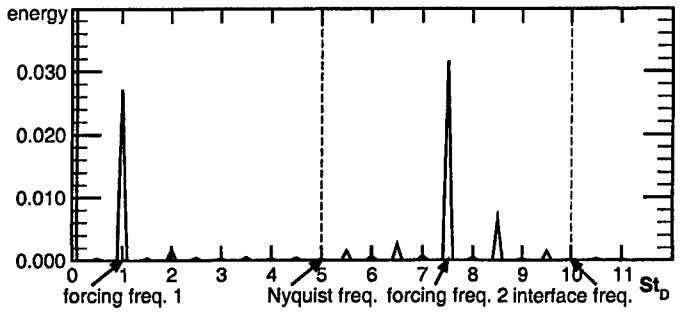

FIGURE 3. Energy spectrum at a point ($x = 2D$, $r = 0.5R$, $\phi = 0$) in the interface plane of the upstream domain.

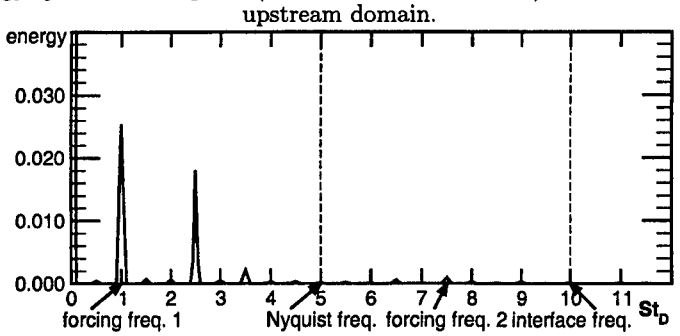

FIGURE 4. Energy spectrum at the interface plane of the downstream domain. Physically identical point as Fig. 3 ($x = 2D$, $r = 0.5R$, $\phi = 0$). No filter used.

has been introduced entirely by the sampling process. Hence, the upstream flow solver has to treat the signal during the sampling process in order to suppress the high frequent perturbation, while keeping the low-frequency oscillation unchanged.

5. Temporal Filters

A common procedure to avoid aliasing errors in experiments is to use low-pass filtering prior to the sampling process. The low-pass filtering suppresses all frequencies above the Nyquist frequency, while passing all lower frequencies unchanged. This filtering process has to be done prior to the sampling process, since otherwise the aliasing error has already taken effect and is indistinguishable from the rest of the long wave spectrum.

To use the same strategy for the sampling of LES data an appropriate digital filter has to be constructed. A digital filter can be defined as:

$$r(t_k) = \sum_{n=0}^{N} b_n s(t_{k-n}) + \sum_{m=1}^{M} a_m r(t_{k-m}) \tag{5.1}$$

with r being the filter response, s the original signal, b_n and a_n the filter constants, and t_k the time. The LES time-step Δt is defined as $t_k - t_{k-1}$. Since in LES computations the time-step is usually not constant, but varies in order to maintain the highest possible time-step satisfying the CFL condition, a pre-sampling process has to be made within. This pre-sampling procedure averages the data with a higher frequency than the actual sampling frequency. In order to avoid aliasing in the pre-sampling process, the frequency of the pre-sampling has to be chosen well within the energy decay, so that the energy of

frequencies higher than the Nyquist frequency are considerably smaller then the energy of the lower frequencies. A filter such as Eq. (5.1) can then be applied.

A filter in the form of Eq. (5.1) uses the history of the signal and the history of prior filter responses. This is a so called infinite response filter (IIR filter), can be used. However, a simplified filter, which uses only the history of the signal, a so called finite response filter (FIR filter) may have advantages:

$$r(t_k) = \sum_{n=0}^{N} b_n s(t_{k-n}) \tag{5.2}$$

First, FIR filters are always stable. Due to the absence of the filter response, no feedback is possible and hence, this kind of filters will cannot amplify errors. Second, FIR filters have a linear phase response. The resulting advantage will be made clear later.

Due to the high number of points at the interface the filter has to be applied to, the order N of the filter is sought to be small, since N determines the number of time-steps that have to be recorded. The determination of the filter constants can be done with any filter design tool such as Matlab (Stearns 2003). The usage of filter design tools allows for the usage of more sophisticated window functions in order to damp the Gibb's phenomenon (Williams 1986), which is most pronounced at filters of low order. For the current investigation, two different filter have been used.

5.1. *Fourier Series Method*

The first filter is designed using the Fourier Series Method (Rorabaugh 1997). The coefficients are defined as:

$$b_n = \frac{1}{2\pi} \int_{2\pi} H(\lambda)[\cos(m\lambda) + j\sin(m\lambda)]d\lambda \tag{5.3}$$

$$\text{with} \quad m = n - \frac{N-1}{2} \tag{5.4}$$

with $H(\lambda)$ being the desired filter response and λ the normalized frequency, which is here normalized to the pre-sampled frequency. The optimal filter response would have a cutoff frequency of $1/2 \cdot f_{\text{interface}}$. The pre-sampling frequency was chosen here twice the interface frequency, which results in a cutoff frequency $\lambda_{\text{cutoff}} = 1/4$. Equation (5.3) then becomes:

$$b_n = \frac{1}{2\pi} \int_{\frac{\pi}{4}}^{\frac{\pi}{4}} \cos(m\lambda)d\lambda + j\frac{1}{2\pi} \int_{\frac{\pi}{4}}^{\frac{\pi}{4}} \sin(m\lambda)d\lambda \tag{5.5}$$

The second integrant is zero, since the integrant is an odd function and the limits of the integration are symmetric. Equation (5.5) then becomes:

$$b_n = \frac{\sin(m\lambda)}{2m\pi}\Big|_{\lambda=-\frac{\pi}{4}}^{\lambda=\frac{\pi}{4}} = \frac{\sin(m\frac{\pi}{4})}{m\pi} \tag{5.6}$$

Note, that the definition of the filters does not include the knowledge of the actual sampling frequency, but only the cutoff frequency relative to the sampling frequency. This means, if the interface frequency is changed, the filters will adapt automatically.

The filter response of this filter is shown in Fig. 5. The dashed line denotes the ideal filter response: below the cutoff frequency it is unity, above zero. Since only a limited number of filter coefficients are available, here $N = 21$, the actual filter response differs from the ideal filter. Most notably, there is an overshoot right next to the cutoff frequency,

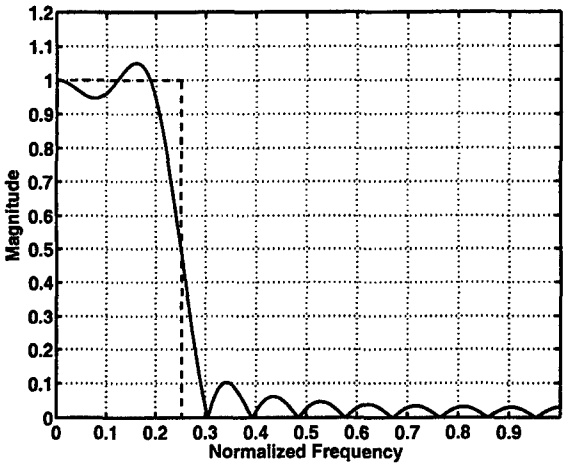

$b_0 =$	$b_{20} =$	0.0311536
$b_1 =$	$b_{19} =$	0.0244766
$b_2 =$	$b_{18} =$	-0.0000006
$b_3 =$	$b_{17} =$	-0.0314696
$b_4 =$	$b_{16} =$	-0.0519226
$b_5 =$	$b_{15} =$	-0.0440576
$b_6 =$	$b_{14} =$	0.0000006
$b_7 =$	$b_{13} =$	0.0734296
$b_8 =$	$b_{12} =$	0.1557666
$b_9 =$	$b_{11} =$	0.2202866
	$b_{10} =$	0.2446776

FIGURE 5. Left: Filter response of filter designed with Fourier Series Method (solid line). $N = 21$. Cutoff frequency: 0.25. Dashed line: Ideal filter response. Right: Filter coefficients

the Gibb's phenomenon. In order to smoothen the filter response a window method has to be employed.

5.2. *Window Method*

The second filter used in this study uses a window method. One of the major shortcomings of the Fourier Series Method is the assumption that the signal is periodic. This creates some problems due to a discontinuity at the end and the beginning of the recorded signal. One possibility to damp this effect is to use window functions:

$$r(t_k) = \sum_{n=0}^{N} b_n w_n s(t_{k-n}) \tag{5.7}$$

with w_n being the window function. Some of the most common window functions are the Hann, Hamming or, Parzen windows. Here, a Kaiser window has been employed (Williams 1986), since this window creates the smoothest filter response (Fig. 6). However, a drawback of window functions is that the slope of the filter response is not as steep as before.

The window function is usually combined with the filter coefficients leading to a new set of coefficients (Fig. 6)

5.3. *Results: Amplitude Response*

In the next step, the filters were applied to the LES computation of the upstream domain. Each filter was applied separately to the LES data in two LES computations. Since the filters have been designed to avoid aliasing, the quality of the signal has been improved.

The signal response of both computations using the two different filters show the desired results (Figs. 7 and 8). The long wave length perturbation at $St = 1.0$, which corresponds to the frequency which is supposed to be transferred, can be found in the downstream domain without a loss of energy. Since the filters have filtered out the high frequency perturbation prior to the actual sampling process, no aliasing can be observed.

These results of both filters show that digital filters are able to suppress aliasing successfully for coupled flow computations. While for the current test case the results of

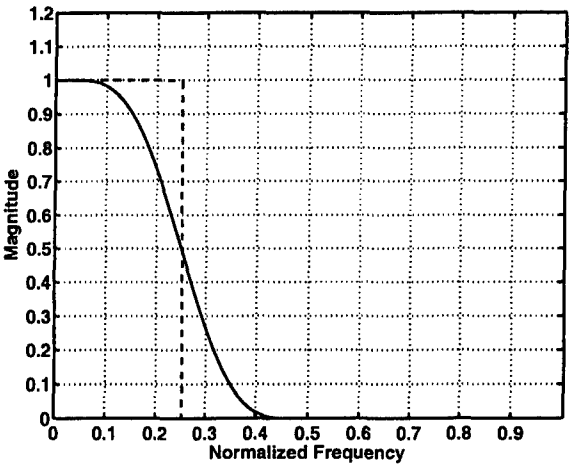

$b_0 =$	$b_{20} =$	0.0004736
$b_1 =$	$b_{19} =$	0.0013386
$b_2 =$	$b_{18} =$	-0.0000006
$b_3 =$	$b_{17} =$	-0.0069236
$b_4 =$	$b_{16} =$	-0.0179856
$b_5 =$	$b_{15} =$	-0.0217416
$b_6 =$	$b_{14} =$	0.0000006
$b_7 =$	$b_{13} =$	0.0583416
$b_8 =$	$b_{12} =$	0.1425086
$b_9 =$	$b_{11} =$	0.2189896
	$b_{10} =$	0.2500006

FIGURE 6. Left: Filter response of filter designed with Window Method (solid line) using a Kaiser window. $N = 21$. Cutoff frequency: 0.25. Dashed line: Ideal filter response. Right: Filter coefficients

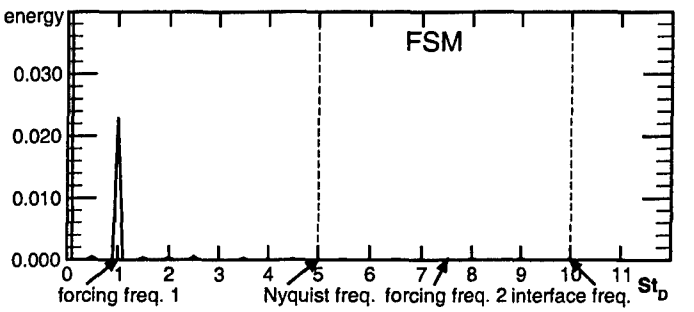

FIGURE 7. Energy spectrum at the interface plane of the downstream domain. Filter designed with FSM (Fig. 5).

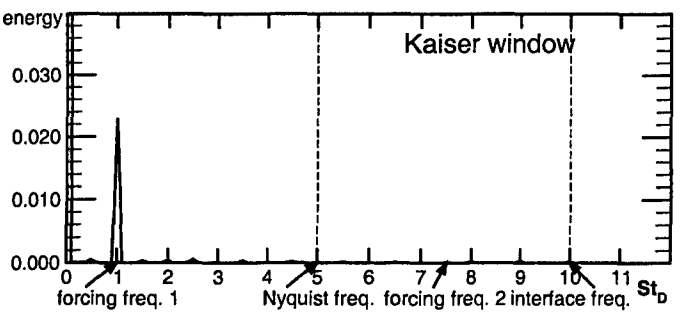

FIGURE 8. Energy spectrum at the interface plane of the downstream domain. Filter designed using Kaiser Window (Fig. 6).

both filters are identical, more complex test-cases may require to choose a filter based on the filter response.

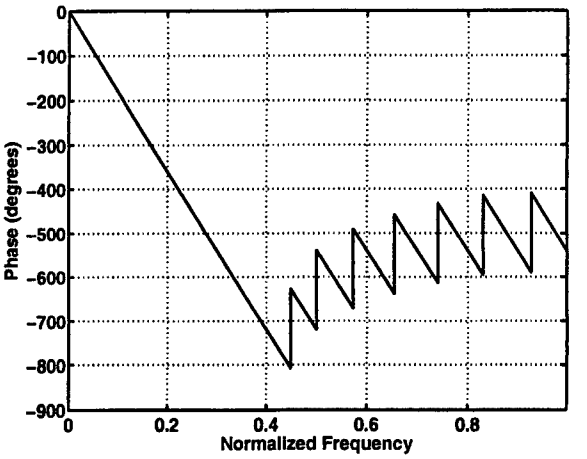

FIGURE 9. Phase response of filter designed with Window Method (solid line) using a Kaiser window. $N = 21$.

5.4. *Results: Phase Response*

Although these filters have shown to efficiently avoid aliasing errors, the application of these filters has a major drawback. Figure 9 shows the phase response of both filters. The phase response is linear in the passing frequency range. This translates to a constant time delay of:

$$\Delta t = \frac{N-1}{2 \cdot f_{\text{sample}}} \tag{5.8}$$

This means that the signal coming from the upstream flow solver arrives with a time delay in the downstream flow solver. The time-delay can be minimized by decreasing the order of the filter. However, it seems that the filters presented here with an order of $N = 21$ are already the minimum order for a filter with an acceptable quality of amplitude response.

If unsteady coupling effects are important, this time delay introduced by the filter is not acceptable.

Since the phase delay is unavoidable using these temporal filters, the application of these filters is limited to the following. Most unsteady RANS flow solvers do not claim to compute a truly unsteady flow, but an ensemble-average or a phase-average. In phase-averaged flows a number of averages of the flow are taken in relation to the phase of a base frequency f_{base}. Assuming that the upstream LES delivers data to a downstream RANS flow solver computing phase-averages, the LES flow solver can compute phase-averages on the basis of the LES data at the interface. Then, a filter is designed which creates the time-delay for one full period of the base frequency. Here, the advantage of a linear phase response of a FIR filter is apparent: the linear phase response translates to a constant time delay, which can be controlled by the order of the filter. The order of the filter is then determined by:

$$N = 2 \cdot \frac{f_{\text{sample}}}{f_{\text{base}}} + 1 \tag{5.9}$$

If the time delay created by the explicit coupling of the flow solvers (Schlüter 2003) can be also corrected in this filter delay, if the order is reduced by 1.

While this procedure might be working for a number of applications, many unsteady LES-RANS computations will neither tolerate the time-delay nor the usage of phase-averages at the interface.

6. Spatial Filters

The major reason why temporal filters are creating a time-delay is the lack of information of the future signal. Since we are interested in single-point time histories, the future development at a given point is given by the flow upstream of this point. Using Taylor's hypothesis:

$$\frac{\partial .}{\partial t} = -u_c \frac{\partial .}{\partial x} \tag{6.1}$$

where u_c is a local convection velocity, time evolutions can be expressed as spatial distributions. The temporal filter then becomes the spatial filter:

$$r(t_k) = \sum_{n=0}^{N} b_n s(x_{k-n}) \tag{6.2}$$

$$\text{with } x_n - x_n - 1 = \frac{u_c}{f_{\text{sample}}} \tag{6.3}$$

Instead of using the time history of the signal, the downstream development is sampled. Unlike the case of the temporal filters, where the time history of the interface points have to be stored, no additional memory is necessary for the spatial form of the filter.

So far, the phase delay is still present, unless the origin of the filter is shifted upstream putting the filter centrally around the desired interface point:

$$x_{0,\text{new}} = x_{0,\text{old}} - \frac{N-1}{2} \frac{u_c}{f_{\text{sample}}} \tag{6.4}$$

Here, the location of the sampling points is defined by the sampling frequency. In many flow solvers, especially when using structured meshes, it may be of advantage to define the sampling frequency according to the mesh spacing. The locations of the sampling points are then defined as points on the mesh and the sampling frequency by the distance of the points:

$$f_{\text{sample}} = \frac{u_c}{\Delta x} \tag{6.5}$$

The advantage of this definition is mainly practical nature, since it is easier to retrieve data from these points. Furthermore, no error due to aliasing in the pre-sampling process is introduced, since the sampling points resolve the entire spectrum on the given mesh.

The disadvantage of this definition of the sampling points is the independence of the sampling frequency from the interface frequency. A variation of the RANS time-step, and hence, a variation of the interface frequency, requires a new definition of the filter, since the desired cutoff frequency has changed, while the sampling frequency remains constant.

For the current study, the spacing of mesh points in axial direction is $\Delta x = 3D/128$. With $u_c = U_{\text{bulk}} = 1.0$ this results in a Strouhal number of $St_{\text{sample}} = 42.67$. The cutoff frequency of $St = 5.0$ results in a normalized cutoff frequency $f_{\text{cutoff}} = 0.117$.

The number of sampling points was limited to $N = 17$. A small number of sampling points is desirable, since the Taylor-hypothesis looses validity with increasing distance to the interface point. Furthermore, the extent of the spatial filter is sought to be small for several reasons. First, in geometries more complex than the current pipe flow, the

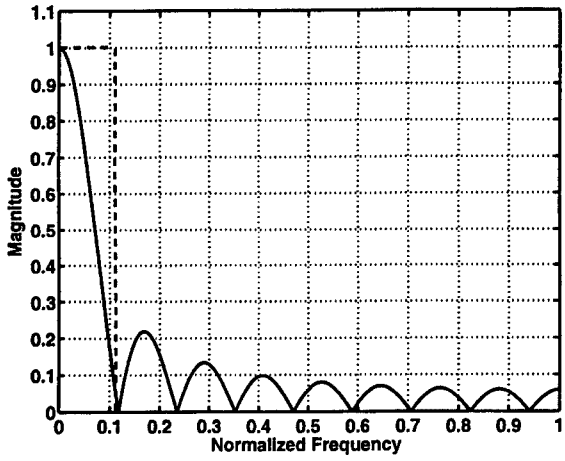

$b_0 =$	$b_{16} =$	0.0588235
$b_1 =$	$b_{15} =$	0.0588235
$b_2 =$	$b_{14} =$	0.0588235
$b_3 =$	$b_{13} =$	0.0588235
$b_4 =$	$b_{12} =$	0.0588235
$b_5 =$	$b_{11} =$	0.0588235
$b_6 =$	$b_{10} =$	0.0588235
$b_7 =$	$b_9 =$	0.0588235
	$b_8 =$	0.0588235

FIGURE 10. Left: Filter response of spatial filter based on a running average (solid line). Dashed line: Ideal filter response. Right: Filter coefficients

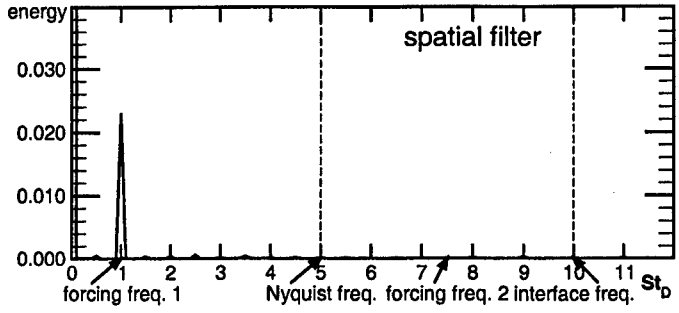

FIGURE 11. Energy spectrum at the interface plane of the downstream domain. Spatial running average filter (Fig. 10).

spatial filter has to be put into an area, where the flow is nearly parallel and has a nearly constant convection velocity over the spatial extend of the filter, which may not be the case over a large portion of the flow. Second, in parallel computations the extend of a spatial filter may be larger than the extend of the flow field computed on a single processor, so that interactions between parallel processors may be necessary.

Since it is rather difficult to design a filter with a low cutoff frequency such as $f_{\text{cutoff}} = 0.117$ on the basis of few sampling points, a running average filter was employed ($b_n = 1/N$). This is the only filter which can ensure that the mean velocity is unchanged. The resulting filter response can be seen in Fig. 10. This filter can still be improved, but seems to be sufficient for the present purposes.

6.1. *Results: Spatial Filter*

The spatial filter was implemented to the upstream LES flow solver computing the pipe flow. The integrated LES-LES computation was performed and the received signal at the inlet of the downstream flow solver examined (Fig. 11). It can be seen that the low frequency perturbation has been transferred correctly. The energy loss due to the filtering is approximately 3%. The high frequency perturbation has been filtered out so that no aliasing errors are present.

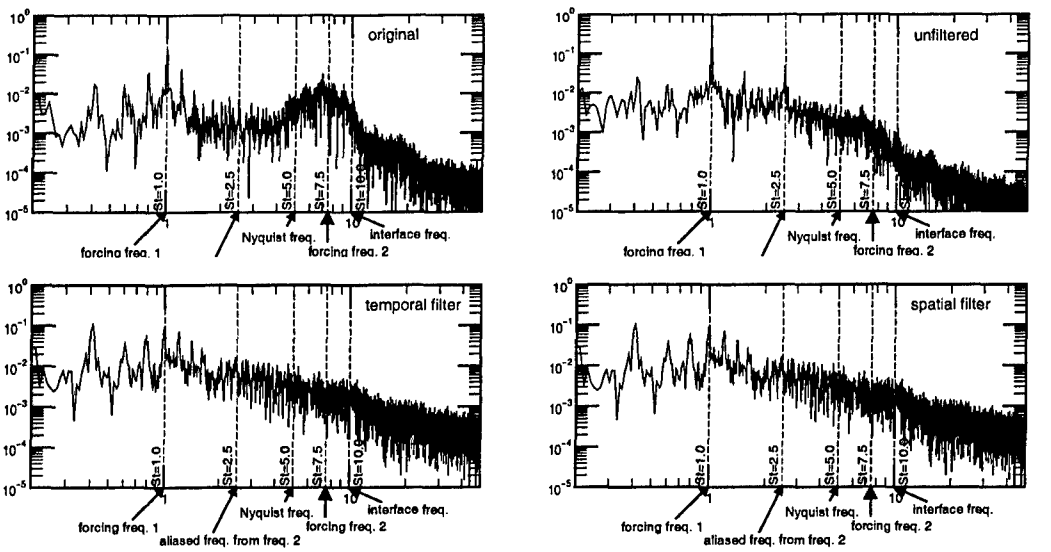

FIGURE 12. Energy spectrum at the interface. Left top: original signal in the upstream domain. Right top: downstream solution without filtering. Left bottom: downstream solution using temporal filter (Kaiser window). Right bottom: downstream solution using spatial filter.

The phase delay of this filter can be expressed as a constant time delay Δt, which is a sum of the filter time-delay and the time correction by the shift of the origin (Eq. (6.4):

$$\Delta t_{\text{total}} = \Delta t_{\text{filter}} + \Delta t_{\text{origin shift}} \tag{6.6}$$

The filter time-delay Δt_{filter} is defined corresponding to Eq. (5.8). The time correction due to the shift of the origin upstream is given by:

$$\Delta t_{\text{origin shift}} = \frac{\Delta x}{u_c} = -\frac{N-1}{2}\frac{u_c}{f_{\text{sample}}}\frac{1}{u_c} \tag{6.7}$$

Equation (6.6) then becomes:

$$\Delta t_{\text{total}} = \frac{N-1}{2 \cdot f_{\text{sample}}} - \frac{N-1}{2}\frac{1}{f_{\text{sample}}} = 0 \tag{6.8}$$

The zero time delay results in a true phase transfer of a given perturbation.

This result shows that anti-aliasing with spatial filters is possible, allowing the proper transfer of amplitude *and* phase of a given perturbations resolved by the Nyquist frequency, and hence, allowing a true unsteady coupling between LES and RANS flow solvers.

7. Turbulent Flows

In order to demonstrate the the filtering procedures on turbulent flows, the computations were repeated using a turbulent pipe flow with a Reynolds-number of $Re = 15,000$. Figure 12 shows the resulting energy spectra for these computations. The upstream spectrum shows two distinct peaks, due to the forcing of the flow. The high frequent perturbation is disturbed by turbulence and the peak is less distinct. Yet, the unfiltered solution shows clearly an aliasing error. The computation using the temporal filter and the spatial filter are both able to suppress aliasing errors.

8. Conclusions

In integrated LES-RANS computations, the higher temporal resolution of the flow in the LES domain may lead to aliasing errors when providing data for a RANS flow solver at lower temporal resolution. This problem is similar to the aliasing problem in experiments, where continuous signals are digitally sampled, and where anti-aliasing is achieved with low-pass filtering prior to the sampling.

It has been shown that the application of a digital low pass filter suppresses aliasing successfully. However, the phase delay introduced by the filter limits the application of temporal filters to phase-averaged solutions.

Using Taylor's hypothesis, the digital filter can be expressed in spatial form. Defining the filter centrally around the desired point allows to obtain a filter without phase delay. Despite some drawbacks, the spatial filter has shown to suppress aliasing successfully, while enabling a true unsteady coupling of flow solvers without phase delay.

The identification of the aliasing problem in integrated LES-RANS computations and its solution using spatial filters is another important step towards unsteady coupled computation of gas turbine engines.

9. Acknowledgments

The support by the US Department of Energy under the ASCI program is gratefully acknowledged.

REFERENCES

AKSELVOLL, K., & MOIN, P. 1996 Large-eddy simulation of turbulent confined coannular jets. *J. of Fluid Mech.*, **315**, 387–411.

CONSTANTINESCU, G., MAHESH, K., APTE, S., IACCARINO, G., HAM, F., AND MOIN, P. 2003 A new paradigm for simulation of turbulent combustion in realistic gas turbine combustors using LES. *ASME Turbo Expo 2003*, GT2003-38356, 2003.

DAVIS, R., YAO, J.,CLARK, J. P. , STETSON, G,ALONSO, J. J., JAMESON, A., HALDEMAN, C., AND DUNN, M. 2002 Unsteady interaction between a transsonic turbine stage and downstream components. *ASME Turbo Expo 2002*, GT-2002-30364, 2002.

GERMANO, M., PIOMELLI, U., MOIN, P. & CABOT, W., 1991 A dynamic subgrid-scale eddy viscosity model. *Phys. Fluids* A **(3)**, 1760-1765.

MAHESH, K., CONSTANTINESCU, G., APTE, S., IACCARINO, G. & MOIN, P., 2001 Large-eddy simulation of gas turbine combustors *Annual Research Briefs 2001* Center for Turbulence Research, NASA Ames/Stanford Univ. 3-18.

MOIN, P., SQUIRES, K., CABOT, W. & LEE, S. 1991 A dynamic subgrid-scale model for compressible turbulence and scalar transport. *Phys. Fluids*, A **(3)**, 2746-2757.

PIERCE, C. D. & MOIN, P. 1998 Large eddy simulation of a confined coaxial jet with swirl and heat release. *AIAA Paper* 98-2892.

C. B. RORABAUGH, 1997 *Digital Filter Designer's Handbook.* McGraw-Hill, 2. edition, 1997.

SCHLÜTER, J., PITSCH, H. 2001 Consistent boundary conditions for integrated LES/RANS simulations: LES outflow conditions. *Annual Research Briefs* Center for Turbulence Research, NASA Ames/Stanford Univ. 19–30

SCHLÜTER, J., SHANKARAN, S., KIM, S., PITSCH, H., ALONSO, J. J., 2002 Integration

of LES and RANS flow solvers: Interface validation. *Annual Research Briefs*, 2002. Center for Turbulence Research, NASA Ames/Stanford Univ.

SCHLÜTER, J. U., 2003 Consistent boundary conditions for integrated LES/RANS computations: LES inflow conditions. *AIAA paper*, (AIAA-2003-3971), 2003. 16th AIAA CFD conference 2003.

SCHLÜTER, J. U., PITSCH, H., AND MOIN, P., 2002 Consistent boundary conditions for integrated LES/RANS simulations: LES outflow conditions. *AIAA paper* 2002-3121

SCHLÜTER, J. U., PITSCH, H., AND MOIN, P., 2003a Boundary conditions for LES in coupled simulations. *AIAA paper*, (AIAA-2003-0069), 2003.

SCHLÜTER, J. U., PITSCH, H., AND MOIN, P., 2003b LES inflow boundary conditions for coupled RANS-LES computations. *submitted for publication to AIAA Journal*, 2003.

SCHLÜTER, J. U., PITSCH, H., AND MOIN, P., 2003c LES outflow conditions for integrated LES/RANS simulations. *submitted for publication to AIAA Journal*, 2003.

SCHLÜTER, J., SHANKARAN, S., KIM, S., PITSCH, H., ALONSO, J. J., 2003d Integration of RANS and LES flow solvers for simultaneous flow computations. *AIAA paper*, (AIAA 2003-0085), 2003.

S. SHANKARAN, M.-F. LIOU, N.-S. LIU, AND R. DAVIS ANF J. J. ALONSO 2001 A multi-code-coupling interface for combustor/turbomachinery simulations. *AIAA paper* 2001-0974

STEARNS, S. D., 2003 *Digital signal processing with examples in MATLAB 2003.* CRC Press, 2003.

D. VEYNANTE AND T. POINSOT 1996 Reynolds averaged and large eddy simulation modeling for turbulent combustion. In *New Tools in Turbulence Modelling*, Les edition physique. Springer, pp 105–140

WILLIAMS, C. S. *Designing Digital Filters.* Prentice-Hall, 1986.